LOAD AND FATIGUE EVALUATION FOR 66KV FLOATING OFFSHORE WIND SUBMARINE DYNAMIC POWER CABLE

Philipp R. **THIES**, Magnus J **HARROLD**, Lars **JOHANNING;** University of Exeter, (United Kingdom),
P.R.Thies@exeter.ac.uk, M.J.Harrold@exeter.ac.uk, L.Johanning@exeter.ac.uk

Konstantinos **GRIVAS**, Georgios **GEORGALLIS;** FULGOR SA, Hellenic Cables, (Greece),
kgrivas@fulgor.vionet.gr, ggeorgal@cablel.vionet.gr

ABSTRACT

Floating Offshore Wind technology has seen a number of prototype deployments around the world in recent years. One of the critical components that must maintain the highest possible integrity is the dynamic power cable. This paper presents the approach and applied methods for the design work that informs the development and qualification of a 66kV submarine dynamic power cable. The design envelope is quantified through coupled aero-hydrodynamic modelling, determining the ultimate load conditions for different cable configurations. The model sensitivity and convergence for an OC4 floating design are explored regarding metocean conditions, computational parameters. A lowered Lazy Wave cable configuration is chosen as most suitable design, providing a compromise between hang-off tensions and induced bending stresses. The numerical results form the basis for subsequent physical cable demonstration and validation tests.

KEYWORD

Dynamic Submarine Power Cable, Floating Offshore Wind, Coupled Analysis; Reliability, Fatigue Evaluation.

1 INTRODUCTION

Floating Offshore Wind technology has matured to a feasible technical solution, with a number of prototype deployments around. Whilst the floating platform type has been variable, all deployments have opted for a horizontal-axis, three-bladed wind turbine. The floating platform types, which have seen full-scale demonstration deployments, include the Spar-buoy, barge and semi-submersible concepts [1].

One of the critical components that must maintain the highest possible integrity to ensure uninterrupted power generation is the dynamic power cable. These dynamic submarine power cables will have to cross the water column, as they typically connect to a subsea connector that provides the link to the static inter-array / export cable.

Floating offshore wind turbines constitute a complex coupled system, comprising of:

- the aerodynamic and structural properties of the turbine blades, nacelle and tower
- the control characteristics of the drivetrain/generator
- the hydrodynamic properties of the floating platform, expressed as Response Amplitude Operators (RAOs)
- the mooring properties and power cable dynamics

It is important to note that each sub-system influences the response of the other sub-system and the overall system response. The dominating aspects are the aerodynamic and hydrodynamic properties, together with the mooring characteristics. The dynamic power cable is designed to avoid an active coupling with the floating platform, thus it will only alter the system behaviour slightly through its additional weight and drag, which are small in comparison to the size and mass of the floater.

The power cable design should be carried out to match the envisaged turbine/platform/mooring arrangement for a specific installation site. Offshore engineering Design standards [2] stipulate a mechanical design assessment that considers the metocean conditions for the Ultimate Limit State (ULS), the Accidental Limit State (ALS) and the Fatigue Limit State (FLS). The work presented here focusses on the ULS condition.

This paper will present the rationale and design work that informs the development and qualification of a 66kV dynamic submarine power cable for Floating Offshore Wind turbines. The paper is structured as follows: First, an overview to the modelling methods and parameters is presented. Second, the results section summarises the numerical convergence and sensitivity, together with the key design drivers and outcomes regarding ULS. The findings are discussed in regarding ongoing and planned development work and related industry developments for floating offshore wind installations.

2 COUPLED NUMERICAL MODELLING

The mechanical load analysis for dynamic submarine power cables is commonly carried out in two distinctive steps:

- A global load analysis that establishes the forces and motions acting on the power cable, induced through the combined effect of the metocean environment and the aero-hydrodynamic response of the floating structure.
- A local analysis that seeks to determine the local stresses (within the cross-section) of the cable, e.g. the stress the armoring or the conductor will have to withstand in operation.

This paper is primarily concerned with the global load analysis. The results thus require a local stress model for the cable in order to estimate the stress acting on each cable layer.

The floating offshore wind turbine assembly, including the turbine, the floating platform, the moorings and the dynamic power cable are modelled using the aerodynamic-hydrodynamic coupling described in [3,4]. This method has been applied for the modelling of non-linear mooring systems [5], as well as the optimization of mooring configurations [6] showing that it provides suitable results in the time-domain [7]. In the following the main features and parameters of each model is briefly outlined.

2.1 Aerodynamic model setup

The aerodynamic model employs the widely-used open access code FAST. A suite of sub-models represents the aerodynamic and structural properties of the wind turbine

and estimates the wind turbine loads in the time-domain [8]. The model employs a reference turbine with a rated capacity of 5MW, see [9] for a complete description.

2.2 Hydrodynamic model setup

The work uses a commercial code [10]. It models offshore engineering design problems through a lumped mass, finite element approach and has been previously applied to dynamic mooring and power cable problems [11, 12].

The analysis has been performed for the semi-submersible platform (OC4), which is described in [13]. Fig. 1 (side view) and Fig. 2 (top view) depict a wireframe overview of the main system components, including the floating semi-submersible platform, maintaining station through three mooring lines at 120 degree spread and the 66kV Dynamic cable with floatation buoys to achieve the Lazy Wave shape in the water column.

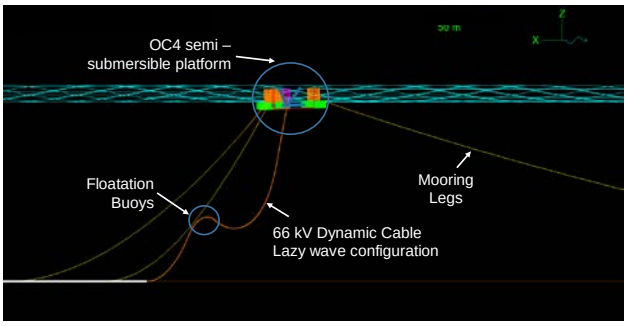

Fig. 1: Overview of platform, cable and mooring configuration

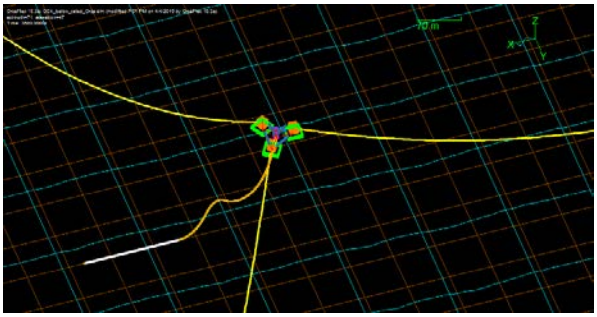

Fig. 2: Top View mooring and cable layout

2.3 Dynamic cable properties

The cross-section and characteristic properties of the modelled 66kV power cable are shown in Fig.3 and Table 1. The cable design adopts a double-armoured, torque-balanced layout with 300mm^2 cross-section copper conductors.

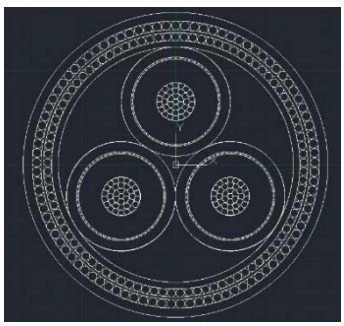

Fig. 3: Cable Cross-section

Table 1: Overview of cable parameters

Parameter [unit]	Symbol	Value
Static axial strength [kN]	F_{max}	71
Rated axial strength [kN]	F_{rated}	300
Minimum bending radius [m]	MBR	2.5

2.4 Environmental Conditions

For the analysis presented here, metocean data from the Wave Hub site in the UK [14] is chosen as notional design site. It should be noted, that the combined wave / water depth and current conditions do not resemble a specific site, but are used to operate a representative model. C:\Users\prt205\Documents\Lecturer\Proposals\Successful\Hellenic Cables\Kostas Work\JI cable. Table 2 summarises the modelled environmental load cases.

Table 2: Overview modelled environmental conditions

Load case	Hs [m]	Tp [s]	V [m/s]
Low rated wind speed	9.0	15	8.0
Medium wind speed	9.0	15	15.0
Upper limit rated wind speed	9.0	15	25.0

3 SIMULATION RESULTS

This section presents the model results in terms of i) convergence and sensitivity, ii) parametric load analysis and iii) model results for the Ultimate Limit State (ULS).

3.1 Numerical convergence and sensitivity

Using the described model setup a range of sensitivity and convergence studies have been performed to consider variations in time step and simulation time. The analyzed time steps included Δt_{Sim1} = 0.0001s; Δt_{Sim2} = 0.001s; Δt_{Sim3} = 0.002s and Δt_{Sim4} = 0.02s. The simulations using Δt_{Sim1} and Δt_{Sim2} produced numerical noise whereas Δt_{Sim3} and Δt_{Sim4} solved with viable results. Comparing the latter two, the mean absolute error MAE = 0.02%, whilst the maximum error was found to be 0.27%. As a result the simulation time step Δt_{Sim4} = 0.02s was selected for all subsequent simulations, balancing computational time and model accuracy.

Five different overall simulation lengths were also assessed regarding model convergence. Table 3 gives an overview of the performed sensitivity studies, observing the change in maximum and mean cable tension, as well as the standard deviation of cable tension (see also Fig 4). The assessed parameters converge towards a steady range after 3,600 s, which was selected as simulation time for all subsequent runs.

Using an Intel R Xeon, 3.2 GHz, 2 cores, 128 GB RAM machine, using simulation parameters (3600 s overall time; Δt_{Sim4} = 0.02s time step) each simulation solved in approximately 12 hours run time, as opposed to 20 hours run time using Δt_{Sim3} = 0.002s.

Table 3: Model parameter sensitivity for varying simulation time

Parameter		Value				
Simulation time [s]	t_{Sim}	300	1200	3600	4800	10800
Max cable tension [kN]	$F_{max, sim}$	46.3	48.4	47.8	49.1	49.2
Mean cable tension [kN]	$F_{mean, sim}$	41.1	41.2	41.2	41.2	41.2
Standard deviation cable tension [kN]	$\sigma_{F, sim}$	2.0	2.4	2.3	2.3	2.3

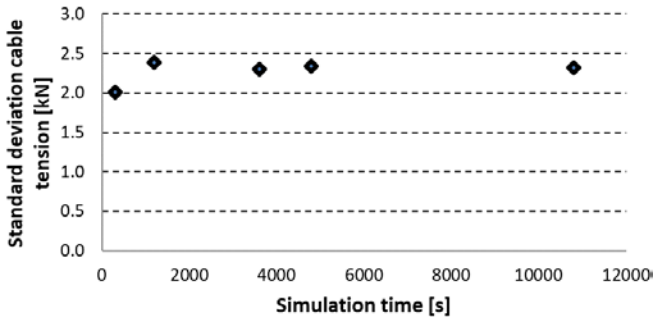

Fig. 4: Variation of cable tension (standard deviation) with different simulation lengths

3.2 Load results

3.2.1 Parametric Analysis for Cable configuration and ULS metocean conditions

Several analysis runs were performed to explore the effect of different Lazy Wave configurations, incident wave direction and wind speeds, under the conditions in Table 2. Three cable configuration, with the Lazy Wave shape at different water depths (peak of Lazy Wave at i) 116m; ii) 135m and iii) 150m) are shown here (see Fig 5).

The results show an interesting trade-off between incurred maximum effective tension and the observed bending radius. Whilst the deep configuration (iii) exhibits the highest effective tension at the hang-off point ($F_{max, iii}$ = 58.2 kN), it has the most favourable bending radius (BR_{iii} = 8.84 m). In contrast, the shallow configuration (i) has the lowest peak tension ($F_{max, i}$ = 41.0kN) but a lower bending radius (BR_{iii} = 5.2m). As a result configuration ii) was chosen as reference design case, balancing the peak tension and bending radius that the cable is subjected to.

For Lazy Wave configuration ii), the wave directionality was varied between 0° and 180°, confirming that the 0° case induces the highest effective tension ($F_{max, 0°}$ 49.47kN) and the lowest bending radius ($BR_{0°}$ 7.14m) for the given metocean parameters.

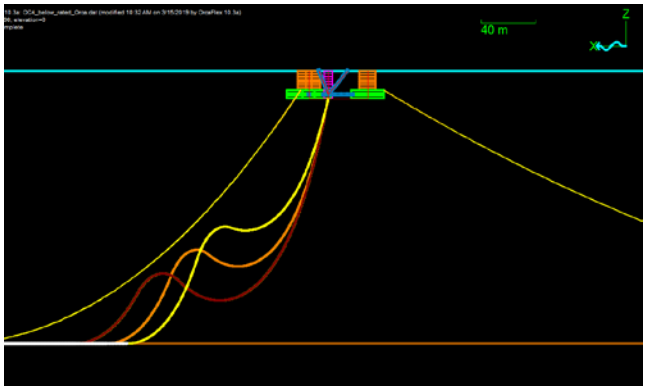

Fig. 5: Lazy Wave cable configurations with flotation buoy depths of i)116m, ii) 135m and iii) 150m; total water depth is D = 200m.

In addition, the effect of different wind speeds (low rated, medium and upper rated wind conditions were evaluated. Table 4 shows that the wind speed has very little influence on the cable tensions or bending radii, indicating that the mechanical cable loads are governed by the incident wave conditions.

The dynamic motion response spectra of the platform for Heave, Surge, Pitch and Roll are shown in Fig 6-9.

Table 4: Overview of parametric analysis, Fixed parameters: Hs = 9 m, Tp = 15s, modelling ULS; t = 3600s; Δt = 0.02s.

Parameter	Effective tension at Hangoff [kN]	Bendig Radius [m]
Lazy Wave shape depth		
i) 116m	41.0	5.2
ii) 135m	49.5	7.14
iii) 150m	58.2	8.84
Wave Direction [°]		
0	49.5	7.14
60	48.6	7.35
120	48.0	7.87
180	47.9	8.06
Wind speed [m/s]		
8	49.5	7.14
15	49.5	7.14
25	49.6	7.30

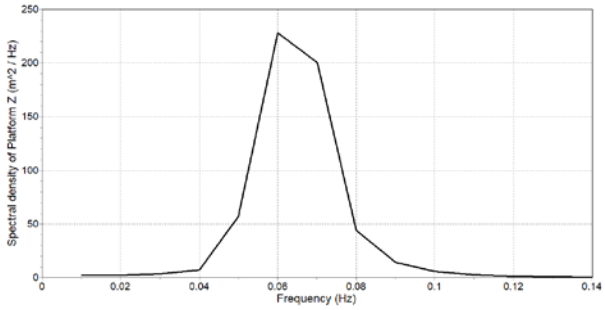

Fig. 6: Dynamic motion response of floating offshore platform – Heave

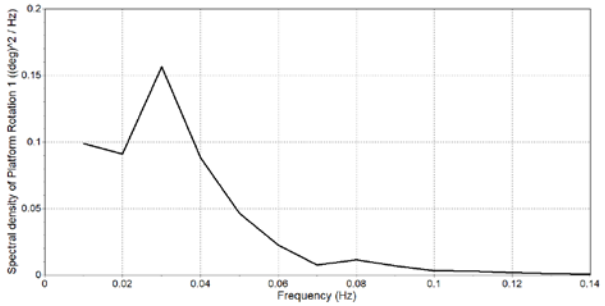

Fig. 7: Dynamic motion response of floating offshore platform - Pitch

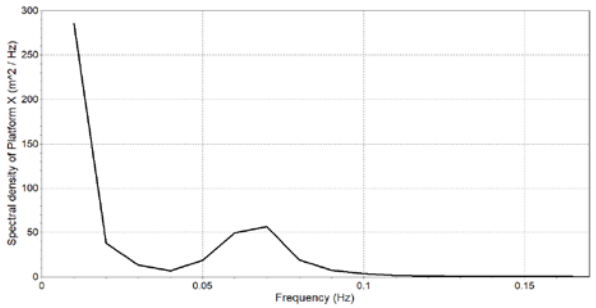

Fig. 8: Dynamic motion response of floating offshore platform – Surge

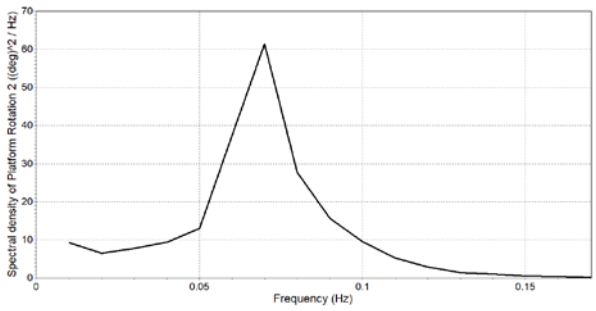

Fig. 9: Dynamic motion response of floating offshore platform – Roll

3.2.2 Ultimate Limit State

Based on the parametric analysis, configuration ii) was chosen for the dynamic cable. The following figures all display the simulation results for the ULS state, i.e. (H_s = 9 m, T_p = 15s, v_{wind} = 8m/s).

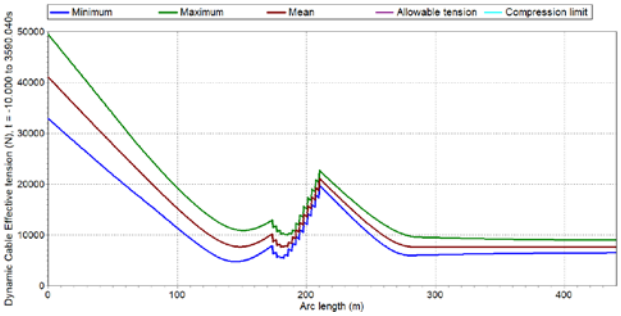

Fig. 10: Range graph plot showing minimum, mean and maximum cable tensions for configuration ii) during ULS simulation (Hs = 9 m, Tp = 15s). Arc length = 0 corresponds to the cable hang off at the platform.

Fig 10. provides an overview of the minimum, mean and maximum tensions observed along the entire length of the cable. Throughout the ULS, configuration ii) does not show any compression (i.e. negative minimum tensions), satisfying an important design criterion. It can be further observed that the highest tension is located at the cable hang off point at the platform (arc length = 0). The tension peak mid-arc (~220m) aligns with the location of the Lazy Wave arc. The visible discrete steps mid-arc, are caused by the discrete floatation buoy elements. The rated axial strength (300 kN) is not reached at any point during the ULS case ($F_{max, ULS}$ = 48kN).

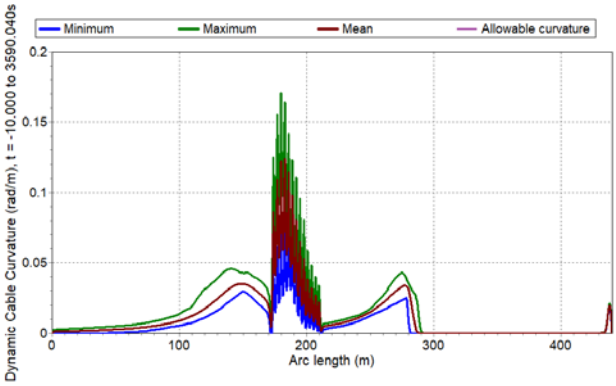

Fig. 11: Range graph plot showing minimum, mean and maximum cable curvatures for configuration ii) during ULS simulation (Hs = 9 m, Tp = 15s). Arc length = 0 corresponds to the cable hang off at the platform. The allowable curvature is κ =0.341rad/m

Fig 11 also displays the entire range of the arc length(x-axis), against the min/mean/max curvature the cable is subjected to during the ULS case. The largest curvature is located at the physical Lazy Wave peak (0.16 rad/m), but is a factor of 2.5 below the rated cable curvature (0.4 rad/m).

Thus, the ULS design criteria regarding tension, compression and MBR constraints are met for the chosen configuration.

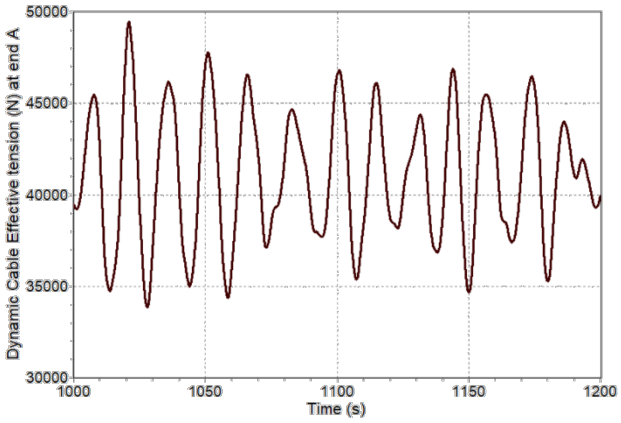

Fig. 12: Time series of cable tension during ULS simulation (Hs = 9 m, Tp = 15s) showing peak tension event at t = 1020s. End A corresponds to the cable hang off at the platform.

The extract time series in Fig. 12 shows the steep, nonlinear tension response of the cable, reflecting the effect of wave groups and incident waves. The ability to estimate the cable response in time domain, will allow a detailed fatigue analysis, once the range of cases for the different metocean conditions is computed.

The motion and displacement envelopes are visualised through the tracer plot in Fig 13. The grey areas denote the motion range during the ULS case. With notable platform and mooring displacements, the compliance of the cable considerably dampens its respective motions.

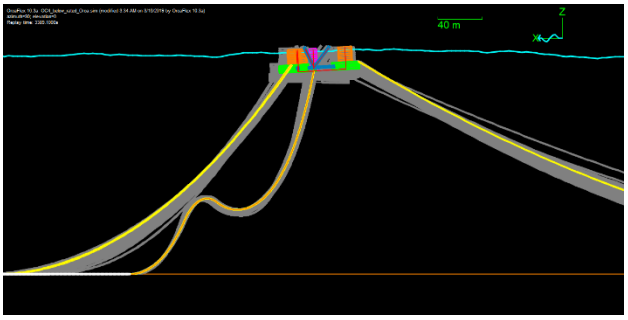

Fig. 13: Illustration of motion envelope (grey traces) for cable configuration ii) during ULS simulation (H_S = 9 m, Tp = 15s).

4 DISCUSSION & CONCLUSION

The paper focusses on the cable design and as such assumes several design assumptions as given. These are themselves coupled and highly site/technology specific. The aerodynamic (wind turbine) and hydrodynamic (floating platform, moorings) model assumptions are themselves complex. However, they are typically available and understood by the technology and platform developer. This paper seeks to emphasize the cable design as an important design consideration, forming part of the overall coupled system. By exploring some of the design configurations, characteristic properties and design parameters of the other sub-systems may be affected, as well as vice versa. Whilst these relationships are not further explored, the presented work forms an important basis in developing this systems engineering approach. Most notable, the motion response of the turbine and platform govern the motion and loads imparted on the cable.

The paper is based on publicly available information regarding the floater and the wind turbine. The size of the turbine (5MW) is relatively 'small' in light of planned developments, with turbine sizes of >7MW A larger turbine and increased mass of the turbine will in turn increase the buoyancy requirements for the floating platform. Both will have an effect on the mechanical cable loads.

The presented study uses site-specific metocean data and findings are thus limited to the chosen load cases. Whilst this provides a suitable baseline model framework, further work will have to explore a range of sites and different floating platform / mooring options.

Subject to further work is also the physical demonstration / validation, which will be completed on a large-scale cable test rig [15], able to carry out force and displacement tests of critical cable sections.

This paper has provided a methodology to assess the cable design for new offshore applications. Once the ULS case is established and the design safety factors are deemed satisfactory, a complete fatigue study is required, performing the full suite of environmental load cases to establish the fatigue life and applicable fatigue safety factors.

Acknowledgments

The first author would like to acknowledge the funding support through the EPSRC Supergen ORE hub 2018, [grant ref EP/S000747/1], https://www.supergen-ore.net/

REFERENCES

[1] IRENA, 2016, "Floating foundations: A game changer for offshore wind power." International Renewable Energy Agency, Abu Dhabi

[2] X. Wang, et al; 2018, "A Review on Recent Advancements of Substructures for Offshore Wind." J. of Energy Conversion & Management, vol. 158, 103-119

[3] NWTC, 2016, "FAST-OrcaFlex Interface." Online, https://nwtc.nrel.gov/OrcaFlexInterface

[4] M. Masciola, et al. 2011, "Investigation of a FAST-OrcaFlex Coupling Module for Integrating Turbine and Mooring Dynamics of Offshore Floating Wind Turbines." Proc. Int. Conf. on Offshore Wind Energy and Ocean Energy. Beijing, China

[5] Harrold M, et al. 2018, "Dynamic Load Reduction and Station Keeping Mooring System for Floating Offshore Wind", Proc. ASME IOWTC2018, San Francisco, USA, 4-7 Nov.

[6] Pillai AC et al., 2018, "Comparing Frequency and Time-Domain Simulations for Geometry Optimization of a Floating Offshore Wind Turbine Mooring System", ASME IOWTC, San Francisco, USA, 4-7 Nov.

[7] Pillai AC et al., 2019, "Impact of Simulation Duration Analysis for Offshore Floating Wind Turbines Using a Coupled FAST-OrcaFlex Model", Proc. ASME OMAE2019, Glasgow, UK, 9-14th June.

[8] J. Jonkman, M Buhl, 2005 "FAST User's Guide." NREL/EL-500-38230. National Renewable Energy Laboratory.

[9] J. Jonkman, et al. 2009, “Definition of a 5-MW Reference Wind Turbine for Offshore System Development.” NREL/TP-500-38060. National Renewable Energy Laboratory

[10] Orcina, 2019. OrcaFlex User Manual: OrcaFlex Version 10.3 b. Daltongate Ulverston Cumbria, UK.

[11] Thies PR, et al., 2012, “Assessing mechanical loading regimes and fatigue life of marine power cables in marine energy applications”, Proc. IMechE, Journal of Risk and Reliability, vol. 226 (1), pp. 18-32.

[12] Thies PR, et al., 2017, “Parametric sensitivity study of submarine power cable design for marine renewable energy applications”, Proc. ASME OMAE2017, Trondheim, Norway, 20 - 25 Jun, OMAE2017-62208.

[13] A. Robertson, et al., 2014 “Definition of the Semisubmersible Floating System for Phase II of OC4”, NREL/TP-5000-60601. National Renewable Energy Laboratory.

[14] Van Nieuwkoop JCC, et al., 2013, “Wave resource assessment along the Cornish coast (UK) from a 23-year hindcast dataset validated against buoy measurements”, Renewable Energy, vol. 58, pp. 1-14.

[15] Thies PR, et al., 2015, “Component reliability test approaches for marine renewable energy”, Proc. IMechE, Journal of Risk and Reliability, vol. 229 (5), pp. 403-416

GLOSSARY

MBR: Minimum Bending Radius
ULS: Ultimate Limit State